Signal Processing 91 (2011) 1143–1149

Contents lists available at ScienceDirect

Signal Processing

journal homepage: www.elsevier.com/locate/sigpro

An L_1 design of GCF compensation filter

Alfonso Fernandez-Vazquez [a,*], Gordana Jovanovic Dolecek [b]

[a] School of Computer Engineering; ESCOM, National Polytechnic Institute; IPN, Mexico City 07738, Mexico
[b] Department of Electronics, National Institute of Astrophysics, Optics, and Electronics; INAOE, Puebla 72840, Mexico

ARTICLE INFO

Article history:
Received 5 November 2009
Received in revised form
28 October 2010
Accepted 1 November 2010
Available online 10 November 2010

Keywords:
CIC filter
GCF
Compensation filter
L_1 optimization

ABSTRACT

This paper introduces the design of the second order GCF (Generalized Comb Filter) compensator based on L_1 optimization. The problem is represented by a set of nonlinear equations solved by the Newton–Raphson algorithm. The proof of the uniqueness of the solution is also provided. One can reduce the complexity of the design approximating the original set of nonlinear equations by the set of linear equations, which depends only on the passband edge frequency ω_p. A design example demonstrates the effectiveness of the proposed design.

1. Introduction

The simplest decimation filter, which requires no multipliers or coefficients storage, is the Recursive Running Sum (RRS), also called Comb filter. Comb filter must have a low passband droop and a high attenuation in the folding bands (bands around the comb zeros), as shown in Fig. 1.

Unfortunately, Comb filter has a high passband droop and a low attenuation in folding bands. There have been proposed different methods for compensating the passband droop as well as for improving the stopband characteristics, for example [1–5].

Recently, a generalization of the Comb filter (GCF) is proposed in [5,6] to improve the attenuation as well as to span the folding bands.

The transfer function of the GCF filter is [5]

$$H_{\mathrm{GCF}_N}(z)=\prod_{m=1}^{N}\frac{\sin(\alpha_m/2)}{\sin(\alpha_m D/2)}\prod_{n=1}^{N}\frac{1-z^{-D}e^{-j\alpha_n D}}{1-z^{-1}e^{-j\alpha_n}}, \tag{1}$$

where α_n, $n=1,\ldots,N$, are rotation parameters, which are optimized to obtain maximum attenuation within folding bands [5]. A useful value for α_n is $\alpha_n=q_n\pi/vD$, where v is an integer factor and q_n is a real value in the range $[-1,1]$, [5].

The corresponding discrete-time Fourier transform (DTFT) of $H_{\mathrm{GCF}_N}(z)$ is

$$H_{\mathrm{GCF}_N}(e^{j\omega})=H(\omega)\exp\left(-j\frac{(D-1)}{2}\left(\omega N+\sum_{n=1}^{N}\alpha_n\right)\right), \tag{2}$$

where

$$H(\omega)=\prod_{m=1}^{N}\frac{\sin(\alpha_m/2)}{\sin(\alpha_m D/2)}\prod_{n=1}^{N}\frac{\sin((\omega+\alpha_n)D/2)}{\sin((\omega+\alpha_n)/2)}. \tag{3}$$

Notice that in general the function $H_{\mathrm{GCF}_N}(z)$ has linear phase characteristics and complex-valued coefficients (see (2)). Using $\alpha_n=-\alpha_{N-n}$, the complex-valued filter coefficients become real-valued [5]. Additionally, Comb filter is obtained by setting $\alpha_n=0$, $n=1,\ldots,N$.

Like the Comb filter, the GCF has a high passband droop. In order to overcome this problem, the authors, in [7,8], propose design techniques for the GCF compensator filter. The optimization uses the following optimally criteria: least square, minimax, and maximally flat.

The least square approach is based on the minimization of the energy error in the pass band region [8]. Unlike the

* Corresponding author.
E-mail addresses: afernan@ieee.org (A. Fernandez-Vazquez), gordana@inaoep.mx (G. Jovanovic Dolecek).

0165-1684/$ - see front matter © 2010 Elsevier B.V. All rights reserved.
doi:10.1016/j.sigpro.2010.11.001

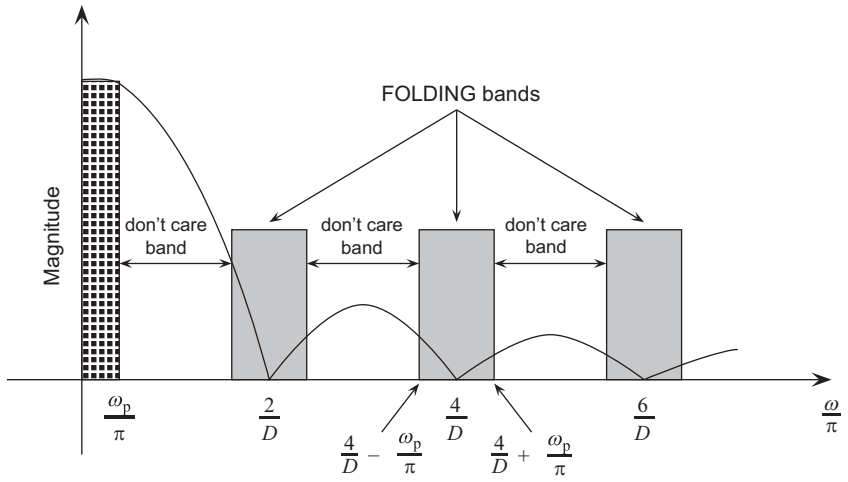

Fig. 1. Magnitude characteristic of the comb filter with decimation factor D.

least square, the minimax approach considers the minimization of the maximum peak ripple [7,8], whereas maximally flat method gives a very flat passband and the filter coefficients of the compensation filter are obtained solving closed form equations [8].

The mentioned optimization methods try only to decrease the passband droop. However, there is no method which considers the decreasing of the peak error ripple in the passband.

The L_1 optimization is considered in [9] to design linear phase lowpass and highpass FIR filters. The resulting L_1 optimal filter possesses the smallest peak error ripple near to the discontinuity. Additionally, the authors provide necessary and sufficient conditions for the uniqueness of the designed filter.

The benefits of the L_1 optimization method give us the main motivation to apply the L_1 optimization for designing passband GCF compensation filter with the minimum peak error ripple.

The rest of the paper is organized as follows. Section 2 introduces the proposed second order compensation filter, while Section 3 presents the L_1 optimization technique. Discussions and results are presented in Section 4.

2. GCF compensation filter

We consider that the proposed GCF compensation filter is given by the following equation:

$$P(z^D) = a + bz^{-D} + az^{-2D}, \tag{4}$$

where a and b are real-valued constants, and D is the decimation factor.

The cascade of the compensation filter and the GCF gives the decimation block structure shown in Fig. 2(a). According to the noble multirate identities [10], the filter $P(z^D)$ can be moved to lower rate resulting in more efficient structure shown in Fig. 2(b).

The resulting overall transfer function is

$$G(z) = H_{\mathrm{GCF}}(z)P(z^D). \tag{5}$$

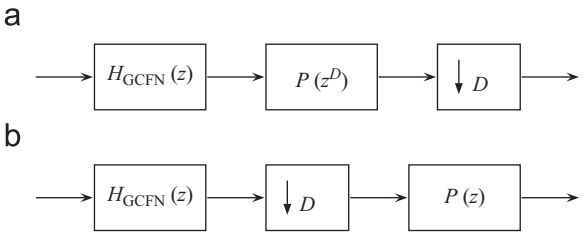

Fig. 2. Decimation block diagrams. (a) Generalized comb filter $H_{\mathrm{GCF_N}}(z)$ and compensation filter. (b) Efficient structure for decimation.

Performing the DTFT and considering $\alpha_n = -\alpha_{N-n}$, Eq. (5) becomes

$$G(\mathrm{e}^{\mathrm{j}\omega}) = \mathrm{e}^{-\mathrm{j}\omega((D-1)N+2D)/2}H(\omega)P_{\mathrm{R}}(D\omega), \tag{6}$$

where $P_{\mathrm{R}}(D\omega)$ is the amplitude response of $P(\mathrm{e}^{\mathrm{j}\omega D})$, which is given by

$$P_{\mathrm{R}}(D\omega) = b + 2a\cos(D\omega). \tag{7}$$

We define the error function in the frequency range $[0,\omega_{\mathrm{p}}]$, where ω_{p} is the passband edge frequency, i.e., the upper edge frequency of the signal band which is necessary to preserve after decimation,

$$E(\omega) = H(\omega)P_{\mathrm{R}}(D\omega) - 1. \tag{8}$$

Combining (7) and (8), we arrive at

$$E(\omega) = H(\omega)(b + 2a\cos(D\omega)) - 1. \tag{9}$$

Let $E(\omega)$ be a function having two simple zeros at $\omega = \omega_1$ and ω_2, where $0 < \omega_1 < \omega_2 < \omega_{\mathrm{p}}$. Consequently, $E(\omega)$ changes sign at the frequency points ω_1 and ω_2. In the following, we investigate the parity of the sign changes. At first, we consider the region $[\omega_2,\omega_{\mathrm{p}}]$. Since ω_{p} is the last frequency point before the transition band and $H(\omega_2)P_{\mathrm{R}}(D\omega_2) = 1$ (see (8)), the parity of $E(\omega)$ for ω in $[\omega_2,\omega_{\mathrm{p}}]$ should be negative. As a result of the sign change at $\omega = \omega_2$ and the parity of $E(\omega)$ in the region $[\omega_2,\omega_{\mathrm{p}}]$, the parity of $E(\omega)$ in (ω_1,ω_2) is positive. Similarly, the parity of $E(\omega)$ in the region $[0,\omega_1)$ is negative.

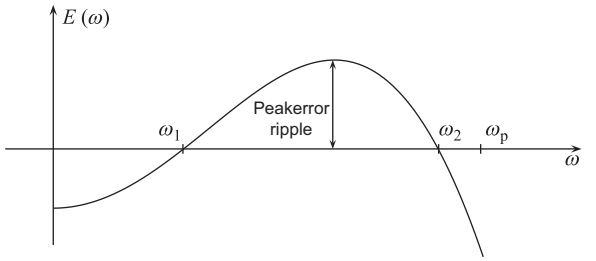

Fig. 3. Error function $E(\omega)$.

Fig. 3 illustrates the error function $E(\omega)$ and the corresponding frequency points ω_1 and ω_2 along with the sign changes. Additionally, as suggested in [9], we define the peak error ripple as the maximum value of $E(\omega)$ before the transition band.

We now compute the values a and b. Considering $E(\omega_1)=0$ and $E(\omega_2)=0$, the following set of linear equation is obtained

$$b+2a\cos(D\omega_1)=1/H(\omega_1), \tag{10}$$

$$b+2a\cos(D\omega_2)=1/H(\omega_2). \tag{11}$$

Solving (10) and (11), we obtain the values of a and b, as

$$a=\frac{1}{2}\frac{1/H(\omega_1)-1/H(\omega_2)}{\cos(D\omega_1)-\cos(D\omega_2)}, \tag{12}$$

$$b=\frac{1}{H(\omega_1)}-2a\cos(D\omega_1). \tag{13}$$

Note that a and b depend on the frequency points ω_1 and ω_2. As a consequence, the problem of finding a and b is reduced to finding the frequency points ω_1 and ω_2. The following section describes the L_1 minimization technique to find the optimum values of ω_1 and ω_2.

3. L_1 optimization

3.1. Problem formulation

The L_1 optimization is expressed as [9]

$$\min_{\omega_1,\omega_2}\varepsilon, \tag{14}$$

where

$$\varepsilon=\int_0^{\omega_p}|E(\omega)|\,d\omega. \tag{15}$$

Substituting (9), (12), and (13) into (15), Eq. (15) results in

$$\begin{aligned}\varepsilon&=-\int_0^{\omega_1}E(\omega)\,d\omega+\int_{\omega_1}^{\omega_2}E(\omega)\,d\omega-\int_{\omega_2}^{\omega_p}E(\omega)\,d\omega\\&=2\int_{\omega_1}^{\omega_2}E(\omega)\,d\omega-\int_0^{\omega_p}E(\omega)\,d\omega\\&=\omega_p-2(\omega_2-\omega_1)+b\left(2\int_{\omega_1}^{\omega_2}H(\omega)\,d\omega-\int_0^{\omega_p}H(\omega)\,d\omega\right)\\&\quad+2a\left(2\int_{\omega_1}^{\omega_2}H(\omega)\cos(D\omega)\,d\omega-\int_0^{\omega_p}H(\omega)\cos(D\omega)\,d\omega\right),\end{aligned} \tag{16}$$

where we have utilized that $E(\omega)$ changes sign at $\omega=\omega_1$ and ω_2.

The necessary condition for ε to have a minimum is

$$\frac{\partial\varepsilon}{\partial\omega_1}=0,\quad \frac{\partial\varepsilon}{\partial\omega_2}=0. \tag{17}$$

After some computations, the following set of nonlinear equations is obtained (details are given in the Appendix):

$$\int_{\omega_1}^{\omega_2}H(\omega)\,d\omega-\frac{1}{2}\int_0^{\omega_p}H(\omega)\,d\omega=0, \tag{18}$$

$$\int_{\omega_1}^{\omega_2}H(\omega)\cos(D\omega)\,d\omega-\frac{1}{2}\int_0^{\omega_p}H(\omega)\cos(D\omega)\,d\omega=0. \tag{19}$$

The geometric interpretation for the choice of ω_1 and ω_2 from (18) and (19) is illustrated in Fig. 4. The area bounded by the graph $H(\omega)$ for ω in $[\omega_1,\omega_2]$ (see first integral in (18)) is the half of the area bounded by the graph $H(\omega)$ for ω in $[0,\omega_p]$ (see second integral in (18)). Similarly, the area represented by the first integral in (19) is the half of the area represented by the second integral in (19).

3.2. Uniqueness of the solution

Suppose that for a given ω_p the frequencies ω_1^* and ω_2^* are solution of the Eqs. (18) and (19). Consequently, from (16), (18), and (19), the minimum value of ε is given by

$$\varepsilon_{\min}=\omega_p-2(\omega_2^*-\omega_1^*). \tag{20}$$

Consider that there exists another solution, i.e., Ω_1 and Ω_2. Using Eq. (20), we write

$$\Omega_2=\Omega_1+\omega_2^*-\omega_1^*. \tag{21}$$

From (18), it follows that

$$\int_{\Omega_1}^{\Omega_1+\omega_2^*-\omega_1^*}H(\omega)\,d\omega=\int_{\omega_1^*}^{\omega_2^*}H(\omega)\,d\omega. \tag{22}$$

However, since $H(\omega)$ is a decreasing function for ω in $[0,\omega_p]$, the value of Ω_1 that satisfies (22) should be ω_1^*. That means that the solution is unique.

As one example, consider that $D=11$, $N=4$, $q_n=[-0.35, -0.83, 0.83, 0.35]$, $v=4$, and $\omega_p=0.4\pi/D$. Fig. 5 shows the objective function ε as a function of ω_1 and ω_2. Note that there is only one minimum defined by ω_1 and ω_2, i.e., $\omega_1^*/\omega_p=0.2877$ and $\omega_2^*/\omega_p=0.7854$.

3.3. Simplification of the solution

Next we express frequencies ω_1 and ω_2 in terms of the passband frequency ω_p. Solving (18) and (19) with the Newton–Raphson method [9], we obtain the frequencies ω_1 and ω_2 as a function of ω_p. Figs. 6 and 7 show plots of ω_1 and ω_2, respectively, for $N=3,4,5,6$, $D=3,5,7,11$, and $v=4$. The values of q_n for different values of N are given in Table 1 [5].

Observe the following

- The relations between ω_1 and ω_p and ω_2 and ω_p are approximately linear in the band $[0,\pi/2D]$.
- The frequency points ω_1 and ω_2 are practically independent of N, D, and v in this band.

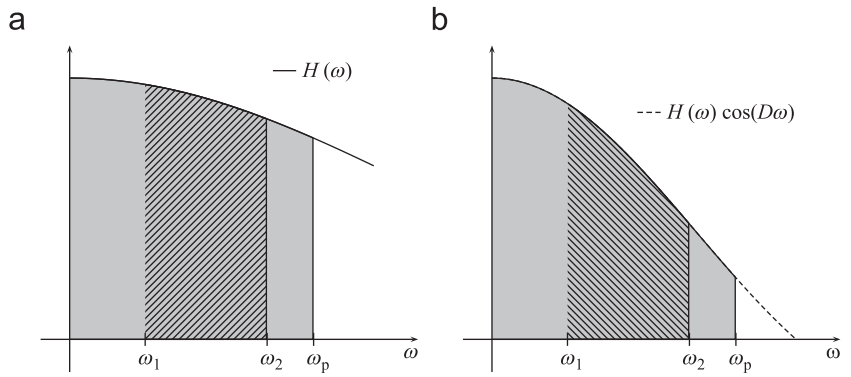

Fig. 4. Geometric interpretation for the selection of ω_1 and ω_2. The dashed area is a half of the area represented by lightgray color.

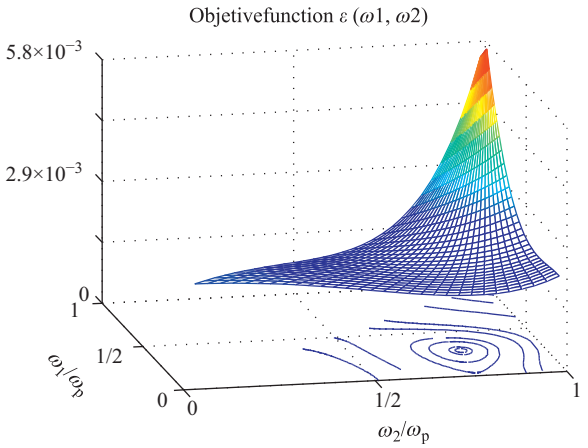

Fig. 5. Objective function ε as a function of ω_1 and ω_2. The parameters are D=11, N=4, q_n=[−0.35, −0.83,0.83,0.35], $v=4$, and $\omega_p=0.4\pi/D$. The minimum value of ε is at $\omega_1^*/\omega_p=0.2877$ and $\omega_2^*/\omega_p=0.7854$.

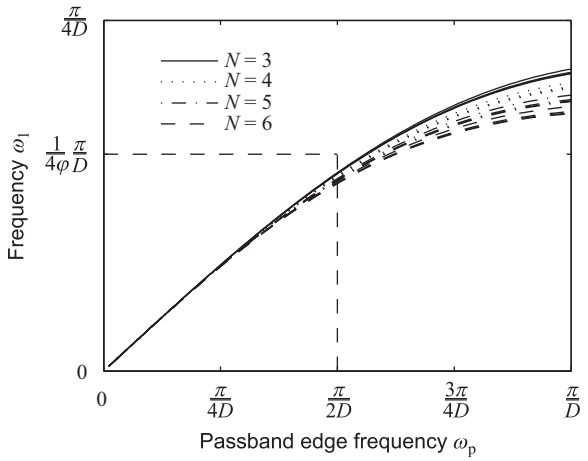

Fig. 6. Frequency ω_1 for L_1 compensation filters as a function of the frequency ω_p, for N=3,4,5,6, D=3,5,7,11 and $v=4$.

In the following, we approximate the values of ω_1 and ω_2 as a linear function of ω_p.

According to (3) the selection $\alpha_n=\alpha_{N-n}$ results in an even function $H(\omega)$. As a result, one can consider the

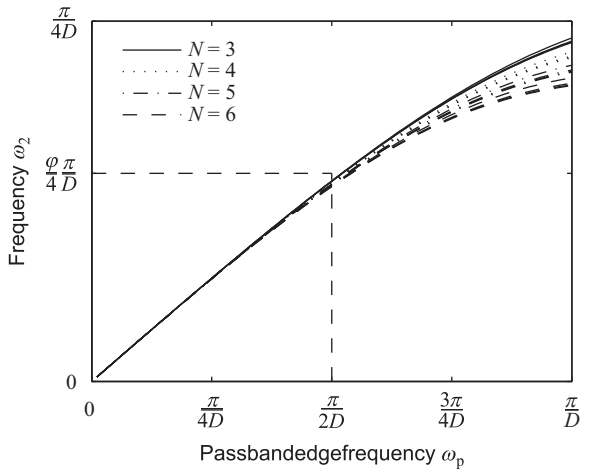

Fig. 7. Frequency ω_1 for L_1 compensation filters as a function of the frequency ω_p, for N=3,4,5,6, D=3,5,7,11 and $v=4$.

Table 1
Different values of q_n.

N	3	4	5	6
q_1	−0.79	−0.35	−0.55	−0.25
q_2	0	−0.88	−0.93	−0.675
q_3	0.79	0.88	0	−0.95
q_4		0.35	0.93	0.95
q_5			0.55	0.675
q_6				0.25

truncated Taylor series of $H(\omega)$ as

$$H(\omega)\approx 1-\frac{H''(0)\omega^2}{2}, \tag{23}$$

where $H''(0)$ is the second derivative of $H(\omega)$ evaluated at $\omega=0$.

In a similar way, for the cosine function we have

$$\cos(D\omega)\approx 1-\frac{D^2\omega^2}{2}. \tag{24}$$

Substituting (23) and (24) into (19) and (18), we arrive at

$$\omega_1\approx\frac{1}{2\varphi}\omega_p,\quad \varphi=\frac{1+\sqrt{5}}{2} \tag{25}$$

$$\omega_2 \approx \frac{\varphi}{2}\omega_p, \tag{26}$$

for ω in $[0,\pi/2D]$.

3.4. Relation with Grossmann and Eldar method [9]

In [9], the authors consider the design of linear phase FIR filters based on L_1 optimization. The necessary and sufficient conditions for the uniqueness of the FIR filter are also provided in the Theorem 4 [9]. The theorem is proved for particular cases, i.e., ideal lowpass and highpass filters.

The error function in [9] is defined as $G(\omega)-1$, where $G(\omega)$ is an FIR filter. However, the error function in our approach is differently defined, i.e., the error function is defined by (8).

The objective function (15) can be rewritten as

$$\varepsilon = \int_0^{\omega_p} H(\omega)\left|P_R(\omega) - \frac{1}{H(\omega)}\right| d\omega. \tag{27}$$

Observe that $H(\omega)$ is a positive function in the band $[0,\omega_p]$. Therefore, according with the Theorem 4 in [9] the unique solution is obtained if and only if $P_R(\omega)-1/H(\omega)$ changes sign two times in $[0,\omega_p]$.

We demonstrated in Section 2 that $P_R(\omega)-1/H(\omega)$ has two sign changes in $[0,\omega_p]$. Consequently, the solution is unique.

4. Discussion of results

In the following we analyze the passband droop R_p in dB after compensation. Fig. 8(a) and (b) illustrate the passband droops as a function of the frequency ω_p, for N=3,4,5,6, D=3,5,7,11, and $v=4$. Observe that the passband droop is less than 0.4 dB in the band of interest.

Now, we compare the proposed L_1 optimization method with the optimization-based methods proposed in the literature [7,8]. Fig. 9 shows the corresponding peak error ripples for the proposed, least square, and minimax designs for N=4,5 and D=3,5,7,9. As expected the proposed design has the smallest peak error ripple.

Design example. We design a GCF compensation filter with the following design parameters D=13, N=5, and $\omega_p = 0.3\pi/D$.

The corresponding passband droop of the GCF filter is $R_p = -0.08$ dB, as shown in Fig. 10. The results of the design are summarized in Table 2.

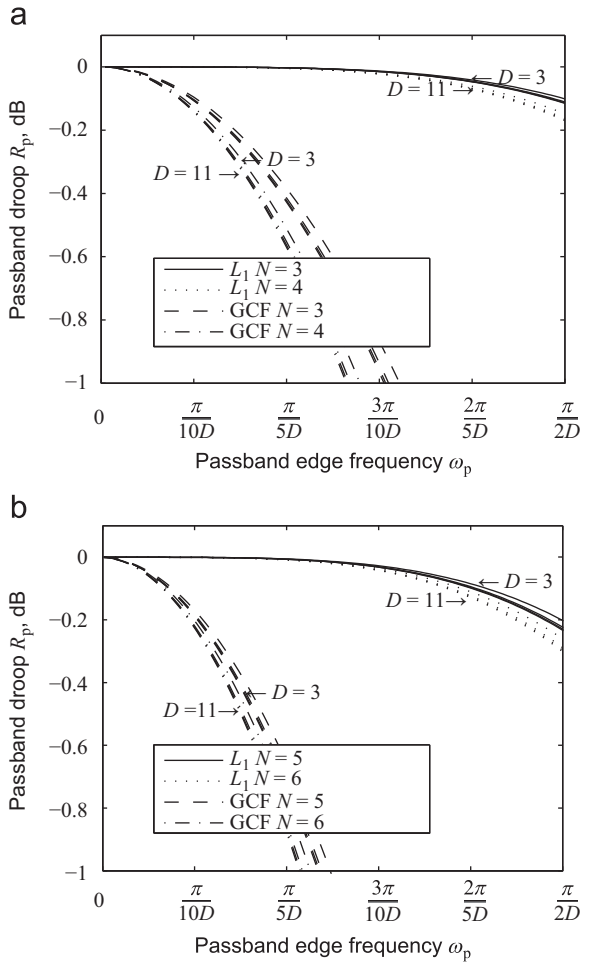

Fig. 8. (a) Passband droops for N=3,4 and D=3,5,7,11. (b) Passband droops for N=5,6, and D=3,5,7,11.

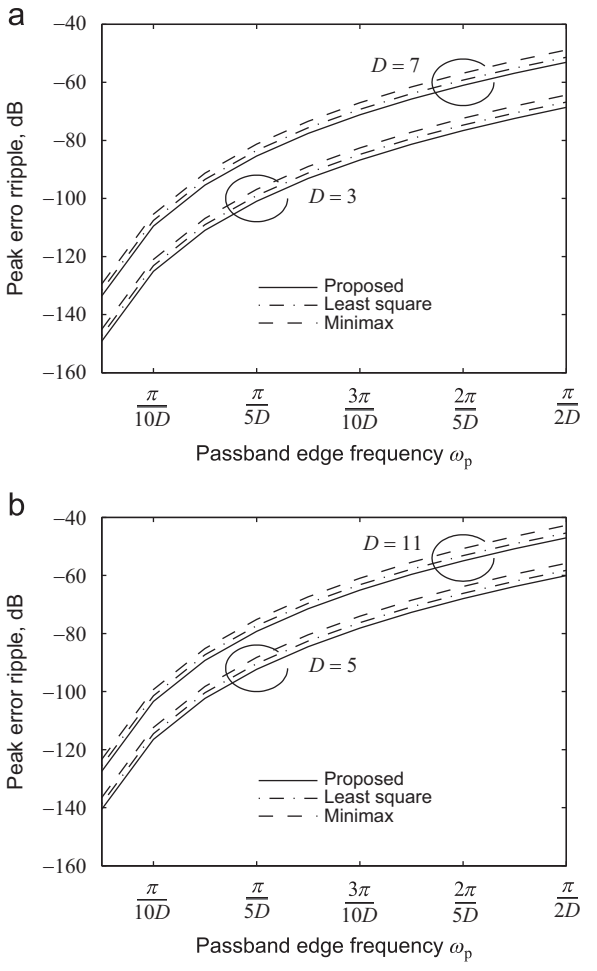

Fig. 9. Maximum ripple as a function of the passband edge frequency ω_p for (a) N=4 and (b) N=5.

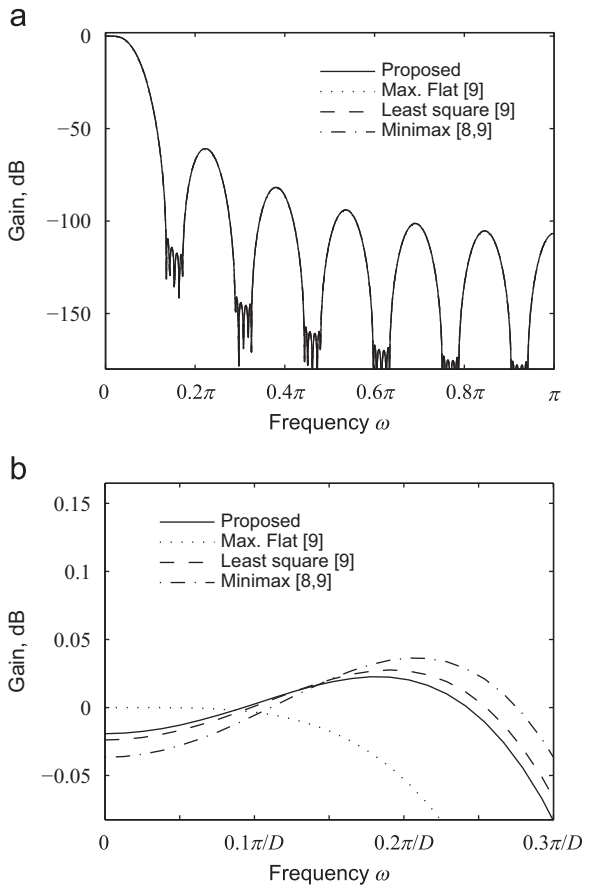

Fig. 10. Overall magnitude response of the GCF filter and the compensation filters in the design example.

Table 2
Parameters in the design example.

	GCF_5	L_1 optimization
R_p	−1.63	−0.08
ω_1		$0.092705\pi/D$
ω_2		$0.242705\pi/D$
a		−0.239975
b		1.477739

The frequency responses along with the passband details are shown in Fig. 10. Additionally, Fig. 10 shows the magnitude responses of the compensations filters using different optimization-based approaches [8,7]. As expected the L_1 approach results in the smallest peak error ripple. However, the cost is a small increase of the passband droop with respect to the other designs.

It is worth noting that the high attenuation of the GCF at the folding bands is not affected. As a consequence, the cascade of the proposed compensator and CGF provides improvement of the passband characteristics as well as high folding bands attenuation.

5. Conclusions

We design a $2D$ order GCF compensation filter, which becomes a second order filter after moving to a lower rate. The coefficients of the filter a and b are obtained using a novel L_1 optimization technique introduced in [9]. In this way, the coefficients a and b are obtained from the set of closed form equations, which depend on the passband edge frequency ω_p. It is worth noting that L_1 optimization approach results in a smallest peak error ripple in the region of interest comparing with other optimization methods like least square and minimax. Furthermore, the cascade of the proposed compensator and CGF provides improvement of the passband characteristics as well as high folding band attenuation. Finally, the proposed design also includes the Comb compensation filter design, as a special case ($\alpha_n = 0$, $n = 1,\ldots,N$).

Acknowledgements

This work was supported by SIP-IPN project 20100636 and CONACyT Mexico.

Appendix

In this appendix we show how to obtain Eqs. (18) and (19).

At first we consider the partial derivatives of b (see (13)), i.e.,

$$\frac{\partial b}{\omega_1} = -\frac{\partial a}{\partial \omega_1}\cos(D\omega_2), \tag{28}$$

$$\frac{\partial b}{\omega_2} = -\frac{\partial a}{\partial \omega_2}\cos(D\omega_1). \tag{29}$$

Now, using Eqs. (28), (29), and the Leibniz rule,

$$\frac{\mathrm{d}}{\mathrm{d}x}\left\{\int_{w(x)}^{z(x)} f(y,x)\,\mathrm{d}y\right\} = f(z(x),x)\frac{\mathrm{d}z(x)}{\mathrm{d}x} - f(w(x),x)\frac{\mathrm{d}w(x)}{\mathrm{d}x} + \int_{w(x)}^{z(x)} \frac{\partial f(y,x)}{\partial x}\,\mathrm{d}y, \tag{30}$$

the partial derivatives of ε are given by

$$\frac{\partial \varepsilon}{\partial \omega_1} = 2\frac{\partial a}{\partial \omega_1}\left(2\int_{\omega_1}^{\omega_2} H(\omega)(\cos(D\omega)-\cos(D\omega_2))\,\mathrm{d}\omega - \int_0^{\omega_p} H(\omega)(\cos(D\omega)-\cos(D\omega_2))\,\mathrm{d}\omega\right), \tag{31}$$

$$\frac{\partial \varepsilon}{\partial \omega_2} = 2\frac{\partial a}{\partial \omega_2}\left(2\int_{\omega_1}^{\omega_2} H(\omega)(\cos(D\omega)-\cos(D\omega_1))\,\mathrm{d}\omega - \int_0^{\omega_p} H(\omega)(\cos(D\omega)-\cos(D\omega_1))\,\mathrm{d}\omega\right). \tag{32}$$

Because ω_1 and ω_2 depend on ω_p, and the partial derivatives of a could be different from zero, Eq. (17) results in

$$\int_{\omega_1}^{\omega_2} H(\omega)(\cos(D\omega)-\cos(D\omega_2))\,\mathrm{d}\omega - \frac{1}{2}\int_0^{\omega_p} H(\omega)(\cos(D\omega)-\cos(D\omega_2))\,\mathrm{d}\omega = 0, \tag{33}$$

$$\int_{\omega_1}^{\omega_2} H(\omega)(\cos(D\omega)-\cos(D\omega_1))\,\mathrm{d}\omega - \frac{1}{2}\int_0^{\omega_p} H(\omega)(\cos(D\omega)-\cos(D\omega_1))\,\mathrm{d}\omega = 0. \quad (34)$$

Subtracting (33) from (34) proves (18). Combining (18) with (34), Eq. (19) holds.

References

[1] K.S. Yeung, S.C. Chan, The design and multiplier-less realization of software radio receivers with reduced system delay, IEEE Trans. Circuits Syst. I 51 (12) (2004) 2444–2459.

[2] S. Kim, W. Lee, S. Ahn, S. Choi, Design of CIC roll-off compensation filter in a W-CDMA digital IF receiver, Digital Signal Process. 16 (6) (2006) 846–854.

[3] G. Jovanovic-Dolecek, S.K. Mitra, Simple method for compensation of CIC decimation filter, Electron. Lett. 44 (19) (2008) 1162–1163.

[4] G. Jovanovic-Dolecek, S.K. Mitra, A new two-stage sharpened comb decimator, IEEE Trans. Circuits Syst. I 52 (7) (2005) 1414–1420.

[5] M. Laddomada, Generalized comb decimator filter for $\Sigma\Delta$ A/D converters: analysis and design, IEEE Trans. Circuits Syst. I 54 (5) (2007) 994–1005.

[6] M. Laddomada, On the polyphase decomposition for design of generalized comb decimation filters, IEEE Trans. Circuits Syst. I 55 (8) (2008) 2287–2299.

[7] A. Fernandez-Vazquez, G. Jovanovic-Dolecek, On the design of GCF compensation filter based on minimax optimization, in: EURASIP 17th European Signal Processing Conference, EUSIPCO 2009, Glasgow, Scotland, 2009, pp. 696–699.

[8] A. Fernandez-Vazquez, G. Jovanovic-Dolecek, A general method to design GCF compensation filter, IEEE Trans. Circuits Syst. II 56 (5) (2009) 409–413.

[9] L.D. Grossman, Y.C. Eldar, An L_1 method for the design of linear-phase FIR digital filters, IEEE Trans. Signal Process. 55 (11) (2007) 5253–5266.

[10] G. Jovanovic-Dolecek (Ed.), Multirate Systems: Design and Applications, Idea Group Publishing, 2002.